Assessing British Columbia Porphyry Fertility Using Zircons

F. Bouzari, Mineral Deposit Research Unit (MDRU), The University of British Columbia, Vancouver, BC, fbouzari@eoas.ubc.ca

C.J.R. Hart, MDRU, The University of British Columbia, Vancouver, BC

Bouzari, F. and Hart, C.J.R. (2019): Assessing British Columbia porphyry fertility using zircons; *in* Geoscience BC Summary of Activities 2018: Minerals and Mining, Geoscience BC, Report 2019-1, p. 45–54.

Introduction

Distinguishing metal-fertile from barren plutons provides a significant advantage to exploration geologists seeking to discover porphyry copper deposits, particularly in British Columbia (BC), where many porphyry systems occur within or around the edges of large batholiths. Zircon ($Zr[Hf]SiO_4$) is a common accessory mineral in granitoid rocks that host porphyry copper deposits. Trace-element composition of zircon is used to determine the age of the rock, temperature and oxidation state of the parental melt. Zircon commonly shows detailed internal texture and zoning, which provide clues to the environment in which it formed and ore-forming processes. The development of stable, rapid, high-resolution geochemical methods of in situ mineral analysis, such as laser-ablation inductively coupled plasma–mass spectrometry (LA-ICP-MS) applied to zircon, has led to an enormous increase in the amount of high-quality isotopic and trace-element data that geochemists and petrologists can access to assist them in resolving problems associated with the geology of igneous and metamorphic rocks (Jackson et al., 2003). Investigations by Ballard et al. (2002) and Shen et al. (2015) correlated the relative uptake of Ce^{4+}/Ce^{3+} in zircon with the oxidation state of barren and fertile porphyry copper-mineralized intrusive rocks in northern Chile and central Asia. Dilles et al. (2015), Lee et al. (2017b) and Banik et al. (2017) showed similar relationships for porphyry copper deposits in Chile and Nevada using the Eu concentration in zircon. Furthermore, Shen et al. (2015) demonstrated a correlation between zircon Ce^{4+}/Ce^{3+} ratios and the size of the porphyry copper deposits in central Asia. These investigations concluded that zircon provides a most useful tool for evaluating the porphyry copper fertility of plutons.

This study investigates district- to batholith-scale fertility indicators of porphyry copper deposits in the Guichon Creek, Takomkane and Granite Mountain batholiths as well as those in the Toodoggone area (Figure 1) by characterizing the textural and geochemical features of zircon to develop tools and strategies for the exploration of porphyry copper deposits in the BC magmatic belts. Results show that the geochemical as well as the textural characteristics of zircon can assist in distinguishing porphyry-fertile plutons from nonmineralized or poorly mineralized plutons.

Zircon for Fertility Studies

Zircon is a preferred heavy mineral to evaluate the potential of plutonic rocks to host porphyry copper deposits because it is a common accessory mineral in a broad range of magmas. Zircon is resistant to subsolidus (hydrothermal) alteration, and demonstrably retains critically important pre-alteration and pre-mineralization geochemical information. Zircon persists in surficial sediments for tens or hundreds of kilometres beyond the hydrothermal or geochemical footprint of magmatic-porphyry centres (Averill, 2011), thus enabling detection of fertile-porphyry clusters at substantial distances from their source and on the regional scale of Cordilleran magmatic provinces (Lee et al., 2017a). Zircon recovery from soil, rock and drillcore samples is both feasible and affordable. Furthermore, in situ U-Pb and Pb-Pb geochronology of zircon using laser ablation has matured to the extent that it constitutes a preferred method to accurately date mineralized and barren magmas (e.g., Stern et al., 2011; Chiaradia et al., 2013).

Geological Setting

The Quesnel terrane in south-central BC is characterized by an Upper Triassic to Lower Jurassic island-arc volcano-sedimentary package with numerous contemporaneous plutons and batholiths, some with associated clusters of porphyry copper deposits (Logan and Mihalynuk, 2014). The plutons and batholiths occur as three arc-parallel belts that progressively young from west to east (Schiarizza, 2015). The western Upper Triassic belt is characterized by the calcalkaline Guichon Creek and Granite Mountain granodioritic batholiths, which host the Highland Valley and Gibraltar porphyry copper districts, respectively (Figure 1). Similar plutonic rock types and potential porphyry copper deposits are expected to occur beneath the Neogene and Quaternary cover rocks. The central plutonic belt consists of the most recent Triassic alkaline plutons that are dominated by monzonitic rocks, including the Copper

This publication is also available, free of charge, as colour digital files in Adobe Acrobat® PDF format from the Geoscience BC website: http://www.geosciencebc.com/s/SummaryofActivities.asp.

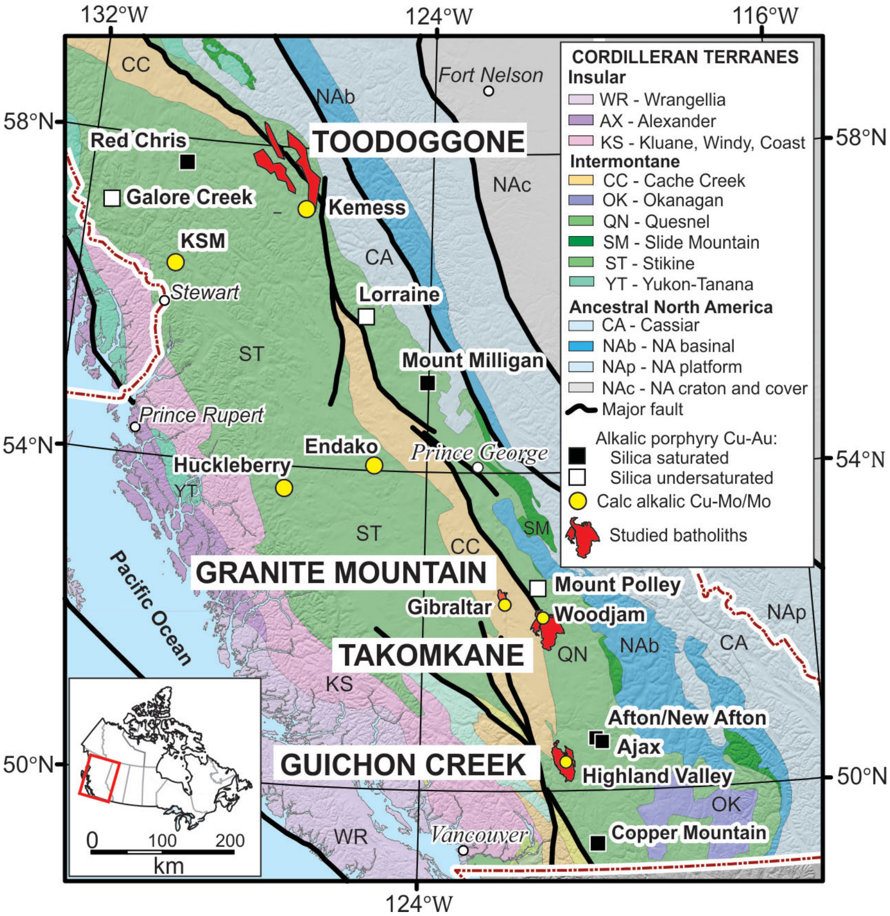

Figure 1. Location map, showing Cordilleran terranes, studied batholiths and major porphyry copper deposits in British Columbia (modified from Bissig and Cooke, 2014).

Mountain, Iron Mask and Mount Polley composite intrusions and related porphyry copper deposits. The easternmost belt consists of several Lower Jurassic calcalkaline granodioritic batholiths such as the Pennask and Takomkane batholiths, which host the Brenda and Woodjam property's Southeast Zone porphyry copper deposits, respectively.

Fertility characteristics of plutons of the Guichon Creek, Granite Mountain and Takomkane batholiths are considered, as well as those of plutons that occur in the Toodoggone area. The geological setting of these areas is provided in Bouzari et al. (2016) and reference therein, a brief summary of each district is given here.

Guichon Creek Batholith

The Upper Triassic Guichon Creek batholith is a north-trending, approximately 65 by 30 km body that intruded and thermally metamorphosed the Upper Triassic Nicola Group basaltic to andesitic volcanic and volcaniclastic rocks (McMillan et al., 2009) of the Quesnel terrane. The batholith is composite and zoned, with earlier diorite and quartz diorite border phases that surround younger granodiorite phases in the centre (Casselman et al., 1995; Byrne et al., 2013; D'Angelo et al., 2017). These mostly concentric phases, from the margins inward, are: the Border phase, the Highland Valley phases (consisting of the Guichon and Chataway subphases), the Bethlehem phases (consisting of the Bethlehem and Skeena subphases) and the Bethsaida phase. The Bethlehem and Skeena subphases and the Bethsaida phase host most of the Highland Valley porphyry copper-molybdenum deposits (Valley, Lornex, Highmont, Alwin, Bethlehem and JA).

Takomkane Batholith

The Takomkane batholith is a large (50 by 40 km) Upper Triassic–Lower Jurassic composite batholith that hosts several mineralized porphyry centres. It intrudes the Upper Triassic Spout Lake pluton and is cut by Lower Jurassic ultramafic–mafic plutons and the Lower Cretaceous Boss Mountain stock. The Takomkane batholith consists of two major units: the Upper Triassic–Lower Jurassic Boss Creek unit and the Lower Jurassic megacrystic Schoolhouse Lake unit. A smaller volume unit of quartz-feldspar porphyry occurs within the Schoolhouse Lake unit. The Woodjam Creek unit is texturally distinct but compositionally similar to the Schoolhouse Lake unit and forms the northwestern part of the batholith (Schiarizza et al., 2009). The Woodjam Creek unit (194.99 ±0.16 Ma, del Real et al., 2017) has a similar age to the Schoolhouse Lake unit but has less quartz and does not contain the large K-feldspar megacrysts that characterize the latter. The Woodjam Creek unit is host to the major porphyry copper deposits, including the Southeast Zone (del Real et al., 2017).

Granite Mountain Batholith

The Upper Triassic Granite Mountain batholith (18 by 10 km), which hosts the Gibraltar porphyry copper mine, occurs near McLeese Lake in south-central BC. The batholith is subdivided into three main units, from the southwest to the northeast: Border phase diorite to quartz diorite, Mine phase tonalite and Granite Mountain phase leucocratic tonalite. The Burgess Creek stock (Panteleyev, 1978), to the northeast, comprises a heterogeneous assemblage of tonalite, quartz diorite and diorite that intrudes the Nicola Group. Mineralization at the Gibraltar mine is hosted in the Mine phase tonalite of the Granite Mountain batholith. The age of the mineralization (215 ±1.0 to 210 ±0.5 Ma), determined based on three dates acquired using the rhenium-osmium method (Harding, 2012), indicates that the mineralization was penecontemporaneous with the emplacement of the Mine phase. But more recent fieldwork (C. Gallagher, pers. comm., 2017) suggests that porphyry dikes that cut the Mine phase were probably more closely associated with the mineralization event than the Mine phase. Samples of these dikes were not available in the course of this study.

Toodoggone Area Plutons

The Toodoggone area in north-central BC is a northwest-trending district located in the eastern part of the Stikine terrane. Geology of the Toodoggone area is described in detail by Diakow et al. (1993, 2005). Asitka, Takla and Hazelton group volcano-sedimentary rocks in the Toodoggone area are intruded by Upper Triassic to Lower Jurassic felsic to intermediate plutons and cogenetic dikes of the Black Lake suite (Diakow et al., 2005). The plutons are exposed at several locations, commonly forming elongated northwest-trending bodies. The Giegerich and Jock Creek plutons occur on the eastern margin of the area and the Duncan Hill pluton occurs in the western and central parts of the area. Small, and probably deeply eroded, porphyry copper mineralization at the Sofia prospect occurs within the Jock Creek pluton. Several smaller and presumably less eroded plutons, such as the Sovereign pluton near the Kemess deposit or those near the Brenda prospect, occur in the central part of the area. Kemess is the major porphyry copper-gold deposit in the district and is associated with the small Maple Leaf granodiorite pluton (Duuring et al., 2009).

Samples and Methods

A total of 127 rock samples were collected from various intrusive phases. Hand-sawn samples were described and further characterized using a petrographic microscope. A subset of 44 samples, representing main intrusive bodies, were selected for zircon separation and analysis, including 12 from the Guichon Creek, 12 from the Takomkane and 7 from the Granite Mountain batholiths, and 13 from the Toodoggone area.

Samples were disaggregated using a Spark 2 electric-pulse disaggregator at Overburden Drilling Management Limited (Nepean, Ontario) to break the rock along mineral-grain boundaries, providing a larger number of unbroken mineral grains. Subsequently, mineral separation was performed at the Mineral Deposit Research Unit, The University of British Columbia using Frantz® magnetic separation and conventional heavy-liquid methods.

Mineral grains were handpicked, mounted and polished in preparation for electron-probe microanalysis (EPMA) and trace-element laser-ablation inductively coupled plasma–mass spectrometry (LA-ICP-MS) at The University of British Columbia. A total of 1022 zircon grains were mounted and analyzed. These grains were studied and characterized by binocular, petrographic and cathodoluminescence (CL) microscopy. Properties such as colour, shape, inclusion populations and zoning were documented for each grain. Mineral grains and spots were then analyzed by EPMA for major elements and some trace elements before being analyzed by LA-ICP-MS for a full trace-element characterization. A total of 1620 spots were analyzed. In the case of smaller grains (<100 µm), one spot was analyzed per sample, whereas for larger grains (>100 µm), two spots were analyzed per grain, one at the grain centre and one at the rim.

Details on the samples and the analytical techniques used in this study will be published in a subsequent publication.

Zircon Texture

Zircon typically forms 100–500 µm long grains with complex internal zoning. Cathodoluminescence imaging was used to characterize the texture of the zircon grains. Oscillatory zoning is the most common type of zoning (Figure 2a), creating zones of green, dark green and grey luminescence. Fine zoning of <1 to >10 µm for each zone is common and occurs around a larger core. Zircon grains locally have a black luminescent core, with an irregular shape resembling an antecryst. Elongated zircon grains display tabular zoning (Figure 2b), which occurs as parallel bands of green, light green, grey or black coloured luminescence; however, fine parallel zoning is not common. A combination of tabular and oscillatory zoning, known as tabular-oscillatory zoning, is also common (Figure 2c) and is characterized by the core of the zircon grains always showing tabular zoning rimmed by oscillatory zoning. However, zircon grains with oscillatory zoning rimmed by tabular zoning were not observed. This relationship suggests that zircons with tabular zoning always formed prior to the zircons with oscillatory zoning. Oscillatory zoning with sector zonation is another common type of zoning (Figure 2d). Zircon grains that show irregular zoning, which commonly occurs in zircon with oscillatory zoning, are distinctly different; in such grains, new growth zones crosscut older zones (Figure 2e, f), thus suggesting that new zircon zones formed by modifying or destroying older zones.

Zircon Trace-Element Chemistry

Zircon trace-element chemistry is a robust tool with which to study magmatic and ore-forming processes. Zircon structure can incorporate many trace elements and because of the slow rates of oxygen diffusion for these elements

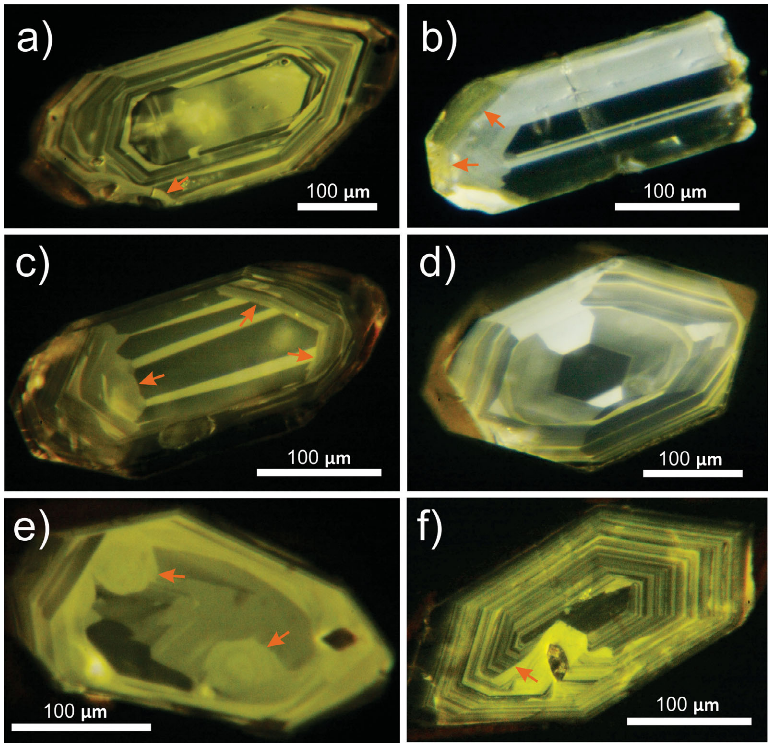

Figure 2. Cathodoluminescence images of zircon grains, showing various types of zoning: **a)** oscillatory zoning in a zircon grain, with some irregular zoning where younger zones crosscut older zones near the rim (indicated by the arrow); **b)** tabular zoning, with oscillatory zoning evident where it started to crystallize near the rim (indicated by the arrows); **c)** tabular zoning rimmed by oscillatory zoning (indicated by the arrows); **d)** oscillatory and sector zoning; **e)** and **f)** irregular zoning with the rim crosscutting the core zoning (indicated by the arrows).

(Cherniak et al., 1997), it retains initial compositions and thus provides a record of magmatic processes occurring during zircon growth such as oxidation state and temperature, which are important factors in the formation of porphyry copper deposits. Zircon in plutonic rocks of the porphyry belts typically display low abundances of light rare-earth elements (LREE) and high relative abundances of heavy rare-earth elements (HREE), with positive Ce and negative Eu anomalies (Ballard et al., 2002; Dilles et al., 2015). Typically, in mineralized intrusions, the Ce anomaly is larger and the Eu anomaly smaller in magnitude compared to nonmineralized intrusions (Ballard et al., 2002).

HREE Enrichment

The Th/U versus Yb/Gd plot shows zircon evolution following a curved path for all batholiths, with the Yb/Gd ratio increasing as the Th/U ratio decreases (Figure 3). The Guichon Creek batholith displays a wide range of Th/U and Yb/Gd ratios for zircons from both nonmineralized and mineralized phases (Figure 3a). However, zircon from the earlier phases, such as the Border and Guichon phases, have high Th/U and low Yb/Gd ratios (>0.45 and <15, respectively), whereas mineralized phases, such as Bethsaida and Skeena, have zircons with lower Th/U and higher Yb/Gd ratios (<0.45 and >15, respectively). Similarly, at the Takomkane batholith, results from zircons recovered from the earlier phases of Spout Lake, Buster Lake and Boss Creek show a curved path, with a wide range of compositions but with higher Yb/Gd and lower Th/U ratios for the Boss Creek relative to the Spout Lake phase (Figure 3b). Zircon composition of the mineralized Woodjam Creek phase, clustered in the middle of the curve, presents a range of Yb/Gd and Th/U ratios strikingly similar to those of the Bethsaida phase of the Guichon Creek batholith. Zircons from the Schoolhouse Lake and quartz-feldspar porphyry phases of the Takomkane batholith appear scattered and fall largely off the main curve (Figure 3b). The zircons from the Granite Mountain batholith follow a similar curve on the Yb/Gd versus Th/U plot (Figure 3c), with the mineralized Mine phase, which occurs in the middle of the curve, displaying similar Th/U ratios to those of zircons from the Guichon Creek and Takomkane batholiths (between 0.2 and 0.45) but slightly lower Yb/Gd (>10). Samples from the Toodoggone area show a similar curved path, with overlap of the Th/U and Yb/Gd ratios of the various phases (Figure 3d). Zircons from the mineralized phases at Kemess and Sofia have low Th/U (<0.5) and high Yb/Gd (>20).

Crystal Fractionation

The increase in Th/U ratios in zircons is attributed to crystal fractionation producing residual melts with relatively high U and Th contents but low Th/U ratios (Miller and Wooden, 2004). The Yb/Gd increase is attributed to apatite, hornblende and titanite crystallization: as the magma cools and crystallizes, apatite, hornblende and titanite fractionation depletes the melt in middle rare-earth elements (MREE), causing an increase in zircon of HREE relative to MREE, and thus high Yb/Gd. The similarity of the Th/U and Yb/Gd ratios of zircons from all mineralized phases suggests that all fertile magmas require a certain amount of fractional crystallization. The variation in zircon compositions along the observed evolutionary paths reflects different proportions of apatite, hornblende and titanite in the sequence of crystallization (Lee at al., 2017b). This is more notable for zircons from the Mine phase of the Granite Mountain batholith that have lower Yb/Gd (10–25), which suggests less fractionated rock. The distribution pattern of the Th/U and Yb/Gd ratios of zircons from the poorly mineralized Schoolhouse Lake and quartz-feldspar porphyry units of the Takomkane batholith is quite scattered and does not follow the curved path of crystal fractionation (Figure 3b), which was probably due to the melts assimilating U-, Th-and REE-enriched crustal materials. Lee et al. (2017b) came to the same conclusion and suggested that poorly mineralized rocks at El Salvador, in Chile, display evidence of crustal mixing and contamination, whereas the mineralized phases show evidence of simple crystal fractionation.

Eu Anomaly and Oxidation State

Europium in magma exists mainly as Eu^{2+}, which prefers partitioning into feldspar and thus generates a negative Eu anomaly in crystalizing zircon. Higher oxidation states promote an increase in the abundance of Eu^{3+}, which favours partitioning into zircon and thus decreases the negative Eu anomaly. The europium anomaly (Eu_N/Eu_N*) is typically calculated as the ratio of chondrite-normalized Eu abundance relative to Sm and Gd. Hafnium is an incompatible element and its content in zircon is used as a proxy for percentage of crystallization and decrease in modal temperature (Dilles et al., 2015). The Eu anomaly versus Hf plot shows distinct variations in BC porphyry-related plutons (Figure 4a–d).

At Guichon Creek, zircons from the nonmineralized Border, Guichon and Chataway phases show an increase in Hf concentration as the Eu anomaly decreases; however, most nonmineralized samples have Eu anomalies <0.3 (Figure 4a). The increase in Hf concentration in zircon occurs as the temperature decreases and magma progressively crystalizes (Dilles et al., 2015). Zircons from the mineralized Bethsaida, Skeena and Bethlehem phases have variable Hf concentrations, with the samples from the Bethsaida and Skeena phases commonly showing higher Hf concentrations than those from the Bethlehem phase, which suggests that the Bethsaida and Skeena phases formed at lower temperatures than the Bethlehem phase. Lee et al. (2017a) reported a similar trend. More importantly, zircons from all three mineralized phases have Eu anomalies >0.35, suggesting that magmatic cooling and crystallization in these mineralized phases occurred under higher oxidation states that prevented the decrease in Eu anomaly values, in sharp contrast to values of the nonmineralized phases.

Zircons from the Takomkane batholith show similar Eu and Hf relationships to those of the Guichon Creek zircons. Samples from the Spout Lake, Buster Lake and Boss Creek plutons show zircons with a wide range of Eu anomalies and Hf concentrations that plot roughly along a curved line (Figure 4b). Zircons from the mineralized Woodjam Creek unit display a distinct Eu anomaly >0.35. Zircons from the younger but nonmineralized phases of the Schoolhouse Lake and quartz-feldspar porphyry units also display similar Eu

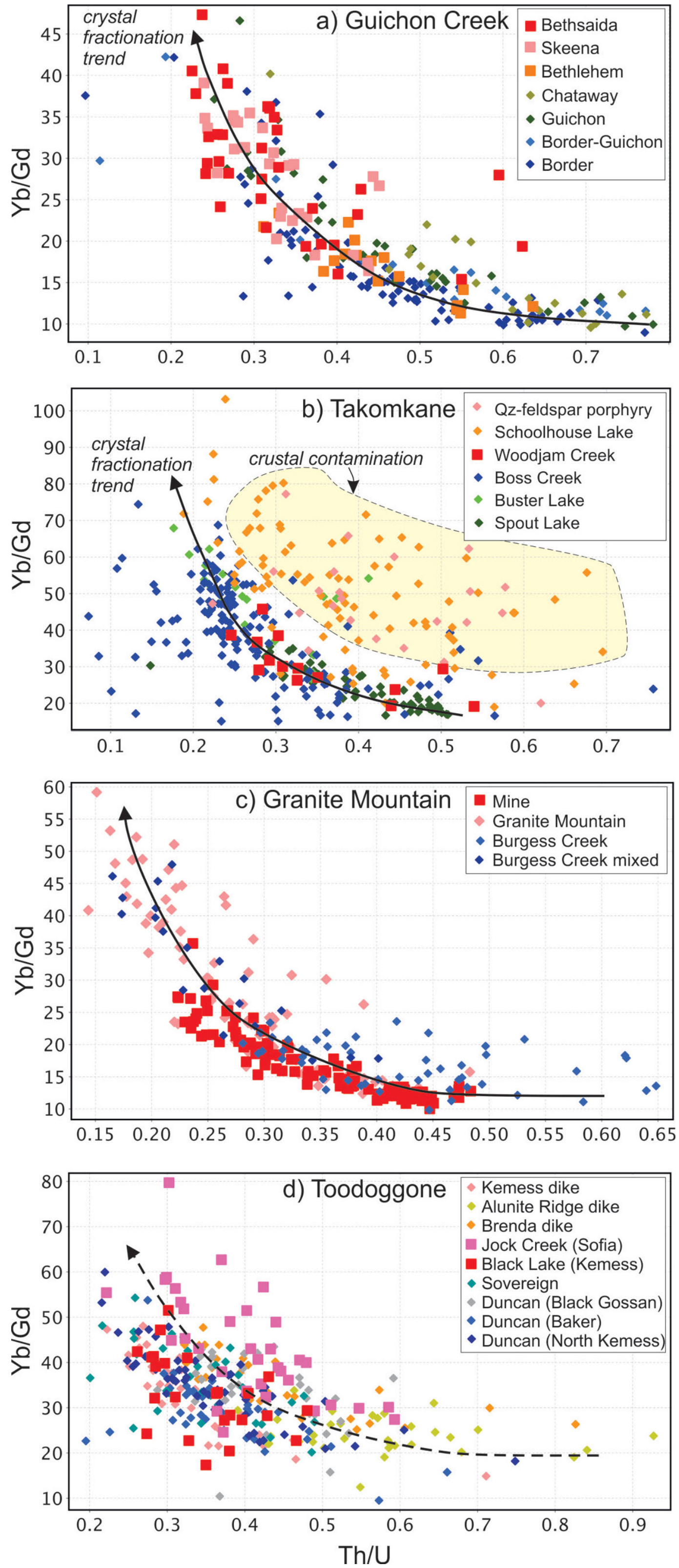

Figure 3. Binary diagram of Th/U versus Yb/Gd, showing a curved evolutionary path for zircons from porphyry-fertile plutons with moderate to high crystal fractionation, along with the scatter plot of plutons with crustal contamination and therefore lacking mineralization: **a)** Guichon Creek batholith; **b)** Takomkane batholith; **c)** Granite Mountain batholith; **d)** Toodoggone area. Abbreviation: Qz, quartz.

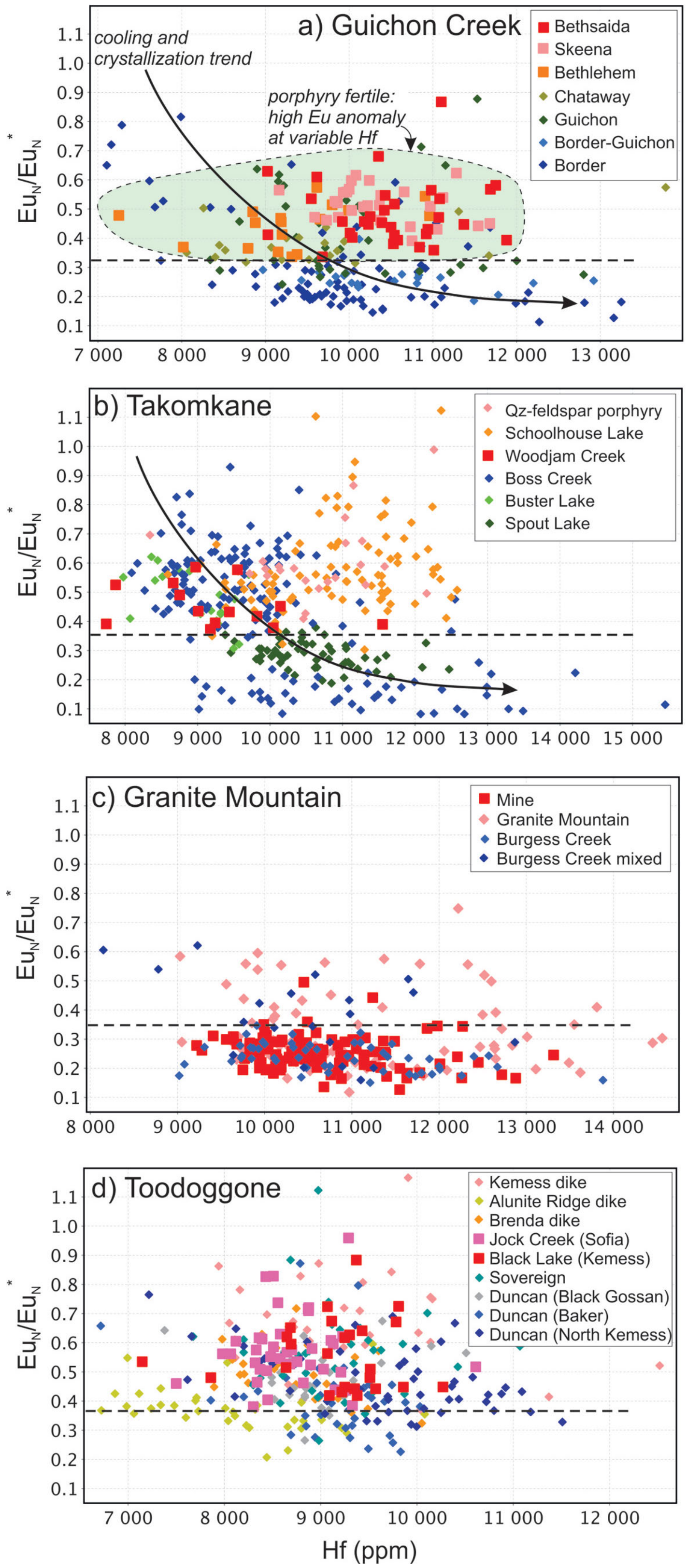

Figure 4. An Eu anomaly (Eu_N/Eu_N^*) versus Hf concentration plot, showing that zircons from mineralized phases have a Eu anomaly >0.35 regardless of Hf concentration, whereas zircons from nonmineralized phases have variable Eu values: **a)** Guichon Creek batholith; **b)** Takomkane batholith; **c)** Granite Mountain batholith; **d)** Toodoggone area. Abbreviation: Qz, quartz.

anomaly values >0.35. However, zircons from these two units show a higher Hf concentration relative to that of the Woodjam Creek unit samples, suggesting that magmas were more fractionated in these younger units.

Zircons from the Granite Mountain batholith show a wide range of Hf concentrations, similar to those from the Guichon Creek and Takomkane batholiths, but the nonmineralized phases and apparently mineralized Mine phase both have zircons with a largely low Eu anomaly (<0.35), which suggests that much of this batholith crystallized under a low oxidation state (Figure 4c). Given the recent field observations on the occurrence of younger mineralized porphyry dikes that cut the Mine phase (see above), it may be that the Mine phase represents a slightly older phase of the mineralization.

Zircon samples from various plutons in the Toodoggone area also show a wide range of Hf concentrations, whereas they commonly show a Eu anomaly >0.35, especially those from the mineralized phase of the Black Lake suite at Kemess and from the Jock Creek pluton at Sofia (Figure 4d). The zircon grains from other phases, such as those from the Duncan and Sovereign plutons, have variable Eu anomaly values ranging from low (<0.35) to high (>0.35).

Effect of Titanite and Apatite Crystallization versus Oxidation State and Magmatic Water

The Eu anomaly is commonly used to characterize the oxidation state of the magma such that at a higher oxidation state most Eu is present in the trivalent state and is not partitioned into fractionating plagioclase (Frey et al., 1978; Dilles et al., 2015). Alternatively, lack of a significant Eu anomaly can also be caused by high magmatic water contents, which suppresses plagioclase fractionation (Richards, 2011). Loader et al. (2017) argued that the fractionation of titanite and apatite has the potential to impart a positive Eu anomaly on residual melts, which may be inherited by zircon when it subsequently crystallizes.

Plots of Eu anomaly in zircon versus Yb/Gd (Figure 5) are used to further characterize the Eu anomaly and the effect of crystal fractionation, oxidation state and magmatic water. As discussed above, the Yb/Gd ratio is a proxy for fractionation of apatite, hornblende and titanite, which depletes the melt in MREE, causing an increase in zircon of HREE relative to MREE (high Yb/Gd). Zircons from the nonmineralized plutons have a wide range of Eu anomaly values (<0.2 to >0.6) and Yb/Gd (~10 to >40).

Zircons from the mineralized plutons, except the Mine phase of the Granite Mountain batholith, display a similar range of Yb/Gd but a distinctly higher Eu anomaly (≥0.35).

The above relationship suggests that apatite and titanite fractionation had different effects on mineralized and nonmineralized plutons. Zircons from the nonmineralized phases of all batholiths show a positive correlation between Yb/Gd and Eu_N/Eu_N* (Figure 5a–d). Thus, as the melt became more fractionated with apatite and titanite (i.e., higher Yb/Gd), the Eu anomaly increased, becoming less negative. Therefore, the increase in the Eu anomaly could have been related to the apatite and titanite fractionation, as described by Loader et al. (2017), although the effect of an increase in oxidation state cannot be ruled out. However, the Eu anomaly values of zircons from the mineralized phases do not show any correlation with Yb/Gd (Figure 5). Thus, the mineralized phases have an Eu anomaly >0.35 whether Yb/Gd ratios are high or low, suggesting that apatite and titanite crystallization did not influence the Eu anomaly in zircons of the mineralized plutons.

The variation in Yb/Gd and petrographic evidence suggest that apatite and titanite fractionation occurred in the mineralized plutons, but the question remains as to why the fractionation processes did not affect the Eu anomaly in zircon? It could be that the effect of apatite and titanite crystallization on the Eu anomaly of zircon was largely minimized or nullified by the high oxidation state and water content of the mineralizing magma.

Correlation Between Trace Element and Zircon Texture

Zircon grains commonly display complex and fine textural zoning (see above). The correlation between these textures and zircon chemistry is usually difficult to establish because of the fine nature of the textural variations in zircon (<10 µm) and the laser-beam size selected for LA-ICP-MS analysis (34 µm in this case). However, this study shows that there is a correlation between the type of zircon grains and their trace-element chemistry. Figure 6a shows the Eu anomaly plotted against Hf content for all studied zircon grains, classified according to their type of zoning. Zircon grains with an elongated shape and tabular zoning distinctly have a lower Eu anomaly, whereas granular zircon grains with oscillatory zoning display a wide range of Eu anomaly values, from low to high, although zircons with a high Eu anomaly (≥0.35) are more common. Zircon grains that display tabular-oscillatory zoning are commonly similar in

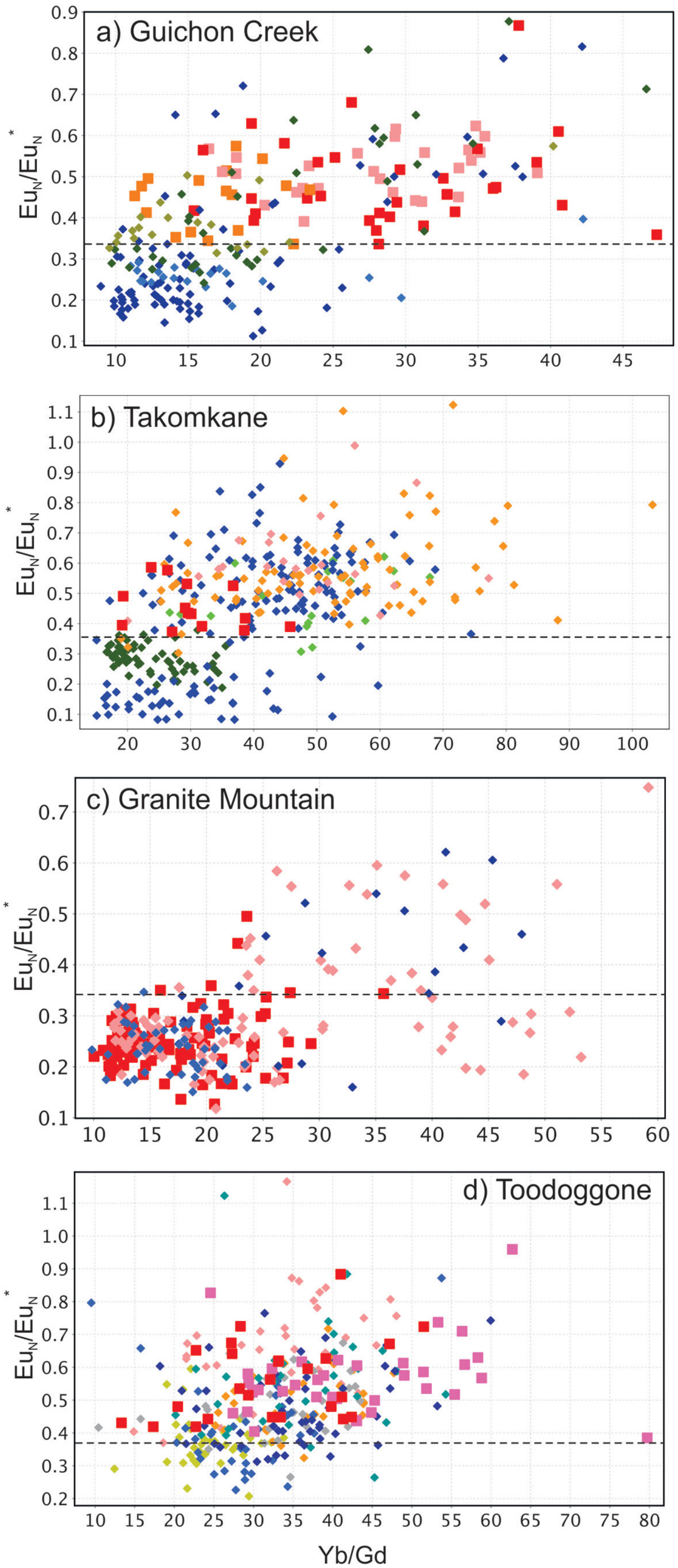

Figure 5. Europium anomaly in zircons and Yb/Gd as a proxy for apatite and titanite fractionation, showing that the Eu anomaly in the mineralized plutons is not affected by apatite and titanite fractionation: **a)** Guichon Creek batholith; **b)** Takomkane batholith; **c)** Granite Mountain batholith; **d)** Toodoggone area. Legend is the same as that used for Figure 4.

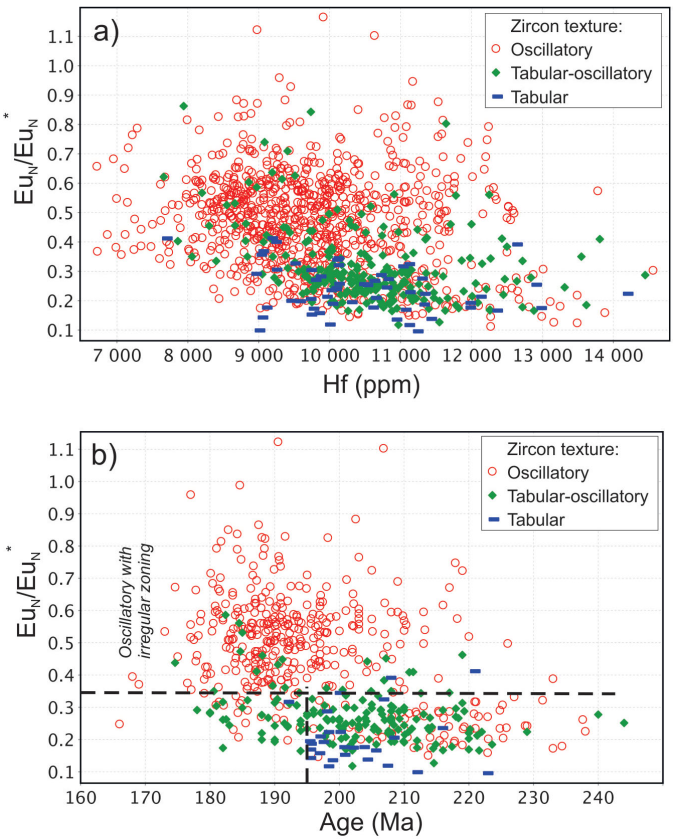

Figure 6. Diagram showing the correlation between zircon texture **a)** and age **b)** with the europium anomaly of zircon.

composition to those with tabular zoning; however, some zircon grains have a composition like that of zircons with oscillatory zoning. The reason for this is that, in the case of most of the grains, the core with tabular zoning was analyzed, whereas in the case of grains rimmed with oscillatory zoning, the rim was analyzed only if was thick enough (>40 µm).

Age calculations based on U-Pb for a subset of grains (Figure 6b) show that zircon grains with tabular zoning and a low Eu anomaly are older than 195 Ma. The zircon grains with oscillatory zoning and a high Eu anomaly have a wide range of ages but are mostly younger than 200 Ma (ca. 180–200 Ma.). This relationship re-emphasizes, as was proposed in McMillan et al. (1995), that the plutons emplaced between 200–185 Ma are more likely to prove fertile. This is particularly true in terms of oxidation state and magmatic water content. More importantly, the shape and texture of zircon grains can be used to screen plutons for fertility since fertile plutons have abundant zircon with oscillatory zoning, which commonly shows irregularities where younger zones crosscut older zones (see above). These preliminary observations suggest that the study of zircon texture can be further developed to help in more efficiently identifying porphyry fertile plutons.

Conclusions

Zircons from the porphyry-fertile plutons in BC show several distinct characteristics that relate them to the ancient magmas that have an increased potential to generate porphyry copper deposits. Zircons from the mineralized plutons have small negative Eu anomalies ($Eu_N/Eu_N^* \geq 0.35$). This reflects 1) high magmatic water content and consequent suppression of early plagioclase crystallization (e.g., Ballard et al., 2002) and 2) late magmatic oxidation resulting in the loss of SO_2-rich magmatic-hydrothermal ore fluids during late-stage crystallization of granite (Dilles et al., 2015; Lee et al., 2017b). In each batholith complex, the mineralized plutons are associated with precursor plutons that are poorly mineralized or nonmineralized. These nonmineralized plutons show a variable Eu anomaly, which is interpreted to be largely controlled by crystal fractionation, particularly that of apatite and titanite (Loader et al., 2017). Therefore, the crystal fractionation of the magmas of these plutons did not produce ore deposits because of a low oxidation state or low magmatic water content, or both. Crystal fractionation also occurred during cooling of the mineralized plutons, but unlike the nonmineralized plutons, the effects of apatite and titanite crystallization were nullified by the high oxidation state and water content of the magma. Therefore, an Eu anomaly distribution in plutons that is not significantly affected by Hf concentration or Yb/Gd values suggests that both magmatic water and oxidation state were high during the entire cooling history of the magma and are potentially a better source of mineralization leading to the formation of porphyry copper deposits.

In summary, the key features of zircon that indicate porphyry-fertile plutons in BC are:

- zircons of Early Jurassic age (ca. 200–185 Ma);
- zircons with oscillatory zoning, particularly the ones that show some irregular zoning patterns crosscutting oscillatory zoning;
- zircons that show simple crystal fractionation, with values on the Yb/Gd versus Th/U plot forming a curved line, which suggests a lack of crustal contamination;
- zircons with an Eu anomaly ≥0.35, which suggests a high magmatic water content and oxidation state; and
- zircons with an Eu anomaly not dependent on Hf concentration or Yb/Gd values, suggesting that magmatic water content and oxidation state were high and remained high during much of the magma crystallization.

Acknowledgments

Geoscience BC is thanked for its financial contribution in support of this project. B. Najafian helped with mineral separation, E. Chan helped with mineral-grain photography and H. McIntyre helped with laser ablation, inductively coupled plasma–mass spectrometry analysis. The authors thank R. Lee of the Mineral Deposit Research Unit, The University of British Columbia for his review of and comments on this paper.

References

Averill S.A. (2011): Viable indicator minerals in surficial sediments for two major base metal deposit types: Ni-Cu-PGE and porphyry Cu; Geochemistry, Exploration, Environment, Analysis, v. 11, p. 279–291.

Ballard, J.R., Palin, J.M. and Campbell, I.H. (2002): Relative oxidation states of magmas inferred from Ce(IV)/Ce(III) in zircon: application to porphyry copper deposits of northern Chile; Contributions to Mineralogy and Petrology, v. 144, p. 347–364.

Banik, T.J., Coble, M.A. and Miller, C.F. (2017): Porphyry Cu formation in the middle Jurassic Yerington batholith, Nevada, USA: Constraints from laser Raman, trace element, U-Pb age, and oxygen isotope analyses of zircon; Geosphere, v. 13, no. 4, p. 1113–1132, URL <https://doi.org/10.1130/GES01351.1> [November 2018].

Bissig, T. and Cooke, D.R. (2014): Introduction to the special issue devoted to alkalic porphyry Cu-Au and epithermal Au deposits; Economic Geology v. 109, p. 819–825.

Bouzari, F., Hart, C.J.R., Bissig, T. and Lesage, G. (2016): Mineralogical and geochemical characteristics of porphyry-fertile plutons: Guichon Creek, Takomkane and Granite Mountain batholiths, south-central British Columbia; *in* Geoscience BC Summary of Activities 2015, Geoscience BC, Report 2016-1, p. 17–22, URL <http://www.geosciencebc.com/i/pdf/SummaryofActivities2015/SoA2015_Bouzari.pdf> [November 2018].

Byrne, K., Stock, E., Ryan, J., Johnson, C., Nisenson, J., Alva Jimenez, T., Lapointe, M., Stewart, H., Grubisa, G. and Sykora, S. (2013): Porphyry Cu-(Mo) deposits in the Highland Valley district, south-central British Columbia; *in* Porphyry Systems of Central and Southern BC, Tour of Central BC Porphyry Deposits from Prince George to Princeton, J. Logan and T. Schroeter (ed.), Society of Economic Geologists, Field Guidebook Series, v. 44, p. 99–116.

Casselman, M.J., McMillan, W.J. and Newman, K.M. (1995): Highland Valley porphyry copper deposits near Kamloops, British Columbia: a review and update with emphasis on the Valley deposit; *in* Porphyry Deposits of the Northwestern Cordillera of North America, T.G. Schroeter (ed.), Canadian Institute of Mining and Metallurgy, Special Volume 46, p. 161–191.

Cherniak, D.J., Hanchar, J.M. and Watson, E.B. (1997): Diffusion of tetravalent cations in zircon; Contributions to Mineralogy and Petrology, v. 127, p. 383–390

Chiaradia, M., Schaltegger, U., Spikings, R., Wotzlaw, J.-F. and Ovtcharova, M. (2013): How accurately can we date the duration of magmatic-hydrothermal events in porphyry systems?–An invited paper; Economic Geology, v. 108, p. 565–584.

D'Angelo, M., Miguel, A., Hollings, P., Byrne, K., Piercey, S. and Creaser, R. (2017): Petrogenesis and magmatic evolution of the Guichon Creek Batholith: Highland Valley Porphyry Cu±(Mo) District, south-central British Columbia; Economic Geology, v. 112, p. 1857–1888.

del Real, I., Bouzari, F, Rainbow, A., Bissig, T., Blackwell, J., Sherlock, R., Thompson, J.F.H. and Hart, C.J.R. (2017): Spatially and temporally associated porphyry deposits with distinct Cu/Au/Mo ratios, Woodjam district, central British Columbia; Economic Geology, v. 112, p. 1673–1717.

Diakow, L.J., Nixon, G.T., Rhodes, R. and Lane, B. (2005): Geology between the Finlay and Toodoggone rivers, Toodoggone river map area, north-central British Columbia (parts of NTS 94E/2, 6 and 7); BC Ministry of Energy, Mines and Petroleum Resources, Open File Map 2005-3, 1:50 000 scale, URL <http://www.empr.gov.bc.ca/mining/geoscience/publicationscatalogue/openfiles/2005/pages/2005-3.aspx> [November 2018].

Diakow, L.J., Panteleyev, A. and Schroeter, T.G. (1993): Geology of the Early Jurassic Toodoggone Formation and gold–silver deposits in the Toodoggone river map area, northern British Columbia; BC Ministry of Energy, Mines and Petroleum Resources, 72 p., URL <http://www.empr.gov.bc.ca/Mining/Geoscience/PublicationsCatalogue/BulletinInformation/BulletinsAfter1940/Documents/Bull86.pdf> [November 2018].

Dilles, J.H., Kent, A.J.R., Wooden, J.L., Tosdal, R.M., Koleszar, A., Lee, R.G. and Farmer, L.P. (2015): Zircon compositional evidence for sulfur-degassing from ore-forming arc magmas; Economic Geology, v. 110, p. 241–251.

Duuring, P., Rowins, S.M., McKinley, B.S.M., Dickinson, J.M., Diakow, L.J., Kim, Y-S. and Creaser, R.A. (2009): Magmatic and structural controls on porphyry-style Cu–Au–Mo mineralization at Kemess South, Toodoggone district of British Columbia, Canada; Mineralium Deposita, v. 44, p. 463–496.

Frey, F.A., Chappell, B.W. and Roy, S.D. (1978): Fractionation of rare-earth elements in the Tuolumne Intrusive Series, Sierra Nevada batholith, California; Geology, v. 6, p. 239–242.

Harding, B. (2012): The characterization of molybdenum mineralization at the Gibraltar mines Cu-Mo porphyry, central British Columbia; B.Sc. thesis, Queen's University, 52 p.

Jackson, S.E., Gunther, D. and Sylvester, P.J. (2003): Applications of laser-ablation ICP-MS analysis: A tribute to Henry P. Longerich; Canadian Mineralogist, v. 41, p. 257–258.

Lee, R.G., Byrne, K., Alfaro, M., D'Angelo, M., Hart, C.J.R., Hollings, P. and Gleeson, S.A. (2017a): Assessing the zircon compositional evolution from the Guichon Creek Batholith and Highland Valley Copper deposit, south-central B.C.; Abstract, Mineral Resources to Discover–14th SGA Biennial Meeting, Québec City, Quebec, August 2017, v. 3.

Lee, R.G., Dilles, J.H., Tosdal, R., Wooden, J.L. and Mazdab, F.K. (2017b): Magmatic evolution of granodiorite intrusions at the El Salvador porphyry copper deposit, Chile, based on trace element composition and U/Pb age of zircons; Economic Geology, v. 112, p. 245–273.

Loader, M.A., Wilkinson, J.J. and Armstrong R.N. (2017): The effect of titanite crystallisation on Eu and Ce anomalies in zircon and its implications for the assessment of porphyry Cu deposit fertility; Earth and Planetary Science Letters, v. 472, p. 107–119.

Logan, J.M. and Mihalynuk, M.G. (2014): Tectonic controls on early Mesozoic paired alkaline porphyry deposit belts (Cu-Au±Ag-Pt-Pd-Mo) within the Canadian Cordillera; Economic Geology, v. 109, p. 827–858.

McMillan, W.J., Anderson, R.G., Chan, R. and Chow, W. (2009): Geology and mineral occurrences (MINFILE), the Guichon Creek Batholith and Highland Valley porphyry copper district, British Columbia; Geological Survey of Canada, Open File 6079, 2 maps, URL <http://geogratis.gc.ca/api/en/nrcan-rncan/ess-sst/78e93fdd-50d0-5877-a024-310362144149.html> [November 2018].

McMillan, W.J., Thompson, J.F.H., Hart, C.J.R. and Johnston, S.T. (1995): Regional geological and tectonic setting of porphyry deposits in British Columbia and Yukon Territory; *in* Porphyry Deposits of the Northwestern Cordillera of North America, T.G. Schroeter (ed.), Canadian Institute of Mining and Metallurgy, Special Volume 46, p. 40–57.

Miller, J.S. and Wooden, J.L. (2004): Residence, resorption and recycling of zircons in Devils Kitchen Rhyolite, Coso volcanic field, California; Journal of Petrology, v. 45, p. 2155–2170.

Panteleyev, A. (1978): Granite Mountain project (93B/8); *in* Geological Fieldwork 1977, BC Ministry of Energy, Mines and Petroleum Resources, BC Geological Survey, Paper 1977-1, p. 39–42.

Richards, J.P. (2011): High Sr/Y magmas and porphyry Cu±Mo±Au deposits: Just add water; Economic Geology, v. 106, p. 1075–1081.

Schiarizza, P. (2015): Geological setting of the Granite Mountain batholith, south-central British Columbia; *in* Geological Fieldwork 2014, BC Ministry of Energy, Mines and Petroleum Resources, BC Geological Survey, Paper 2015-1, p. 19–39, URL <http://www.empr.gov.bc.ca/Mining/Geoscience/PublicationsCatalogue/Fieldwork/Documents/2014/02_Schiarizza.pdf> [November 2018].

Schiarizza, P., Bell, K. and Bayliss, S. (2009): Geology and mineral occurrences of the Murphy Lake area, south-central British Columbia (NTS 093A/03); *in* Geological Fieldwork 2008, BC Ministry of Energy, Mines and Petroleum Resources, BC Geological Survey, Paper 2009-1, p. 169–188, URL <http://www.empr.gov.bc.ca/Mining/Geoscience/PublicationsCatalogue/Fieldwork/Documents/2008/15_Schiarizza.pdf> [November 2018].

Shen, P., Hattori, K., Pan, H., Jackson, S. and Seitmuratova, E. (2015): Oxidation condition and metal fertility of granitic magmas: zircon trace-element data from porphyry Cu deposits in the Central Asian orogenic belt; Economic Geology, v. 110, p. 1861–1878.

Stern, C.R., Skewes, M.A. and Arevalo, A. (2011): Magmatic evolution of the giant El-Teniente Cu-Mo deposit, central Chile; Journal of Petrology, v. 52, p. 1591–1617.